

Interactions between MoS₂ nanotubes and conventional additives in model oils



A. Tomala^a, M. Rodríguez Ripoll^{a,*}, C. Gabler^a, M. Remškar^b, M. Kalin^c

^a AC2T Research GmbH, Wiener Neustadt, Austria

^b Institut "Jožef Stefan", Ljubljana, Slovenia

^c Laboratory for Tribology and Interface Nanotechnology (TINT), University of Ljubljana, Slovenia

ARTICLE INFO

Keywords:

Nanoparticles
Additives
Friction
Wear

ABSTRACT

The use of transition metal dichalcogenides nanoparticles is an emerging concept in lubrication for enhancing the tribological properties of lubricants. However, in fully-formulated products other properties are essential for providing a comprehensive protection against degradation. Therefore, the coexistence of nanoparticles with conventional additives is unavoidable. The main objective of this work is to investigate the tribological performance of MoS₂ nanotubes accompanied by anti-wear, extreme pressure, detergents and dispersants. The results shown synergetic interactions between MoS₂ nanotubes with anti-wear and detergents additives, slight synergy with extreme-pressure additives and antagonistic interactions with dispersants. Under extreme pressure conditions all selected additives provide synergistic effects with MoS₂ nanotubes. The interaction mechanisms are investigated using several techniques and discussed in terms of tribofilm chemistry.

1. Introduction

The tribological properties of engine and gearbox lubricants have a significant impact on efficiency of vehicles, as they reduce friction in a variety of contacts, and protect surfaces from wear [1,2]. The use of nanoparticles as lubricant additives has proved to enhance the tribological properties of surfaces in relative motion [3]. The recent breakthroughs in nanoparticles synthesis [4–6] allows scaling-up the technology for industrial applications. Thus, prospects of nanoparticles such as Inorganic Fullerene-like (IF-) molybdenum disulfides (MoS₂) in lubricant additivation, with excellent friction and wear reducing properties are growing rapidly.

Current additives contain various elements or chemical groups (e.g. S, P, Cl or metals in organic complexes), which release toxic compounds or greenhouse gasses upon degradation. As a consequence, successive regulations constantly require the reduction of the Zn, S and P content in lubricants and fuels. Although it may be impossible to eliminate completely the use of all these elements, it may be feasible to reduce their use by combining them with NPs or compounds with a reduced impact on the environment. Most of the NPs that have been investigated contain simple elements and are more environmentally-friendly [7]. Furthermore, the synthesis of NPs is usually focused on simple reactants, unlike existing additives (i.e. zinc dialkyl dithiophosphate), which require toxic chemicals such as P₂S₅ and CS₂ [8]. Used

in green lubricants (i.e. lubricants manufactured, used and disposed in an environmentally responsible manner), NPs have the potential to replace toxic additives in future lubrication technologies [7].

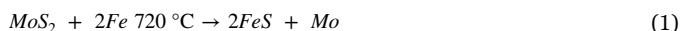
The tribological potential of MoS₂ nanoparticles for automotive applications has been a subject of interest in recent years [9–12]. However, when intending to use NPs in fully formulated lubricants, the presence of other coexisting additives can influence their performance dramatically [10,13,14]. It is reported in [10] that IF-MoS₂ nanoparticles lost their lubricating abilities when added to fully formulated lubricants, due to the presence of dispersants, which prevented nanoparticles from forming tribofilms on the rubbing surfaces. This fact is due to excessive adsorption of the dispersants on the released MoS₂ platelets and/or the steel surfaces, which prevent tribofilm adhesion. On the other hand, the paradigmatic anti-wear additive zinc dialkyl dithiophosphate (ZDDP) has also been investigated in combination with WS₂ [13,14]. The authors observed a synergistic effect between the two additives tested in PAO oil at 100 °C, i.e. the ZDDP/WS₂ mixture generated ~5 times less wear than 1 w/w% ZDDP and ~25% less friction than 1 w/w% WS₂. It was concluded that WS₂ enhances the antiwear properties of ZDDP, while ZDDP protects WS₂ particles from oxidation and increases their friction reducing properties. In a similar work, it was found that MoS₂ nanoparticles having different morphologies and chemistries had a synergistic effect with ZDDP pre-formed tribofilms [1]. Transmission electron microscopy

* Corresponding author.

E-mail address: Manel.Rodriguez.Ripoll@ac2t.at (M.R. Ripoll).

images highlighted that the reason for this was that MoS₂ nanoparticles exfoliated on top of ZDDP tribofilms, enabling easy shear.

The formation of additive derived tribofilms in tribological contacts is a dynamic process which depends on the reactivity of the additives (towards the substrate and between themselves) and the operating conditions (temperature, time, load, slide-roll ratio etc.) [15,16]. This is especially the case for antiwear (AW), extreme pressure (EP) and nanoparticle additive mixtures, which compete to react/adsorb on the rubbing ferrous substrates. The generation of tribofilms is the result of the simultaneous interaction of these additives with the surface of the wear track. The presence of S in the structure of transition dichalcogenides such as WS₂ and MoS₂ enables these additives to display an EP behavior under favourable conditions [17]. Some studies have analysed the chemical composition of the wear tracks generated by MoS₂ and found traces of elemental Mo, which can occur by the following chemical reaction [18,19]:



This reaction with the Fe substrate was found to occur above 720 °C, leading to the formation of elemental Mo and iron sulphide FeS. Such temperatures are possible at asperity contacts under extreme pressure conditions and therefore, the iron sulphide formed on the asperities can prevent metal contact and seizure. It was proposed that the tribological properties of MoS₂ are due to both a mechanical effect (i.e. acting as an efficient friction modifier and separating the surfaces) and a chemical effect (i.e. acting as an EP additive by the formation of iron sulphides in the contact) [18].

This study aims to delineate the effect of conventional additives, such as anti-wear additives, extreme pressure additives, detergents and dispersants on MoS₂ nanotubes performance using various experimental techniques. The dispersion analysis showed that the additives affect the nanotubes distribution in the lubricants: extreme-pressure additives, detergents and dispersants improve the dispersion in the oil, while NTs alone and in the presence of ZDDP form clusters. NTs clusters are easier to trap in point contact, while in line contact the dispersion itself does not seem to be an issue concerning NTs effectiveness, however it does concerning tribochemistry in the contact.

The tribological results show synergetic interactions between MoS₂ nanotubes with selected AW additives, extreme pressure and detergents, moderate with selected EP additives and antagonistic interactions with selected dispersants.

2. Experimental section

2.1. Materials

2.1.1. Test specimens

The test specimens used for SRV® tribological tests were AISI 52100 steel balls and discs, of hardness 850 HV10 and roughness Ra 0.05 µm. The specimens were cleaned before the tests in ultrasonic bath first with toluene (10 min) and then with petroleum ether (10 min).

The test specimens used for Brugger tribological tests were AISI 52100 steel friction ring (Ø=25 mm) with hardness of 60 HRC and roughness Ra < 0.8 µm and a test cylinder (Ø=8 mm) with hardness of 65 HRC and roughness Ra < 0.2 µm.

2.1.2. Lubricants and nanoparticles

The base oil used in this study was PAO 4 having a viscosity of 24.6 mm²/s at 40 °C and 4 mm²/s at 100 °C. The zinc dialkyl dithiophosphate ZDDP used had a primary alkyl structure, with 99% purity, and was obtained from Lukoil Lubricants Europe (Vienna, Austria). Sulphurized olefin polysulphide (40% of sulphur content) was used as the EP additive, and was obtained from Lukoil Lubricants Europe (Vienna, Austria). Succinimide dispersant (based on long chained hydrocarbon amines with 2000 molecular weight) and overbased Ca-

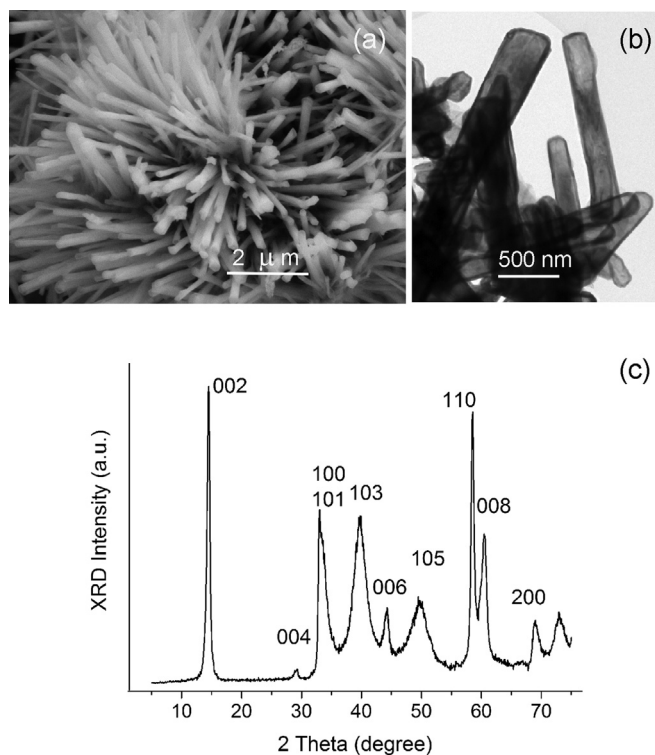


Fig. 1. MoS₂ nanotubes: a) SEM micrograph; b) TEM micrograph; c) XRD pattern assigned according to 2H-MoS₂ (JCPDS-77-1716).

sulfonate detergent were obtained from Infineum International Ltd.

The nanotubes (NTs) investigated in this study were synthesized from Mo₈S₂I₈ nanowires by the procedure reported in [4] at 1073 K in a reactive gas composed of 98 vol% Ar, 1 vol% of H₂S and 1 vol% of H₂ for 1 h. The pristine MoS₂-NTs kept the original, hedgehog self-assembly [2] of the starting material, which can be easily dispersed in polar media using ultrasound. The diameter of the NTs is in a range 100–150 nm (Fig. 1a and b), while their length is up to 3 µm. The walls of the NTs are approx. 10 nm thick and form dome terminations. The X-ray diffraction spectrum (Fig. 1c) revealed a pure MoS₂ compound, which is assigned according to 2H polytype of MoS₂ (JCPDS-77-1716).

The fluids were blended into mixtures using additive concentrations of 2% or 5% by weight depending on the type of additive, and NTs concentration 5% by weight applying an ultrasonic processor VC 505 Sonics & Materials, Inc. This ultrasonic processor is designed for small volume applications (250 µl–1 l), the ultrasonic vibrations at the probe tip were set to 20% amplitude for 8 min, while the pulse was on for 2 s followed by 2 s pulse off.

The base oil used and additives used in this study were blended into following mixtures (Table 1):

Table 1
Overview of the mixtures MoS₂ nanotubes mixtures with selected oil additives.

Blend designation	MoS ₂ nanotubes	Additive
PAO	-	-
PAO+NTs	5%	-
PAO+AW	-	2% ZDDP
PAO+AW+NTs	5%	2% ZDDP
PAO+EP	-	2% EP
PAO+EP+NTs	5%	2% EP
PAO+disp	-	5% Dispersant
PAO+disp+NTs	5%	5% Dispersant
PAO+det	-	5% Detergent
PAO+det+NTs	5%	5% Detergent

- (a) additive-free poly- α -olefin (PAO4) base oil, reference lubricant – referred as PAO
- (b) PAO4 with 5% nanotubes (NTs) – referred as PAO+NTs
- (c) PAO4 with 2% ZDDP (zinc dialkyl dithiophosphate) anti-wear additive – referred as PAO+AW; same mixture additionally blended with 5% nanotubes – referred as PAO+AW+NTs
- (d) PAO4 with 2% active sulphurized olefin 40%S extreme-pressure additive – referred as PAO+EP; the same mixture additionally blended with 5% nanotubes – referred as PAO+EP+NTs
- (e) PAO4 with 5% succinimide dispersant – referred as PAO+disp; the same mixture additionally blended with 5% nanotubes – referred as PAO+disp+NTs
- (f) PAO4 with 5% overbased Ca-sulfonate detergent – referred as PAO+det; the same mixture additionally blended with and 5% nanotubes – referred as PAO+det+NTs

2.2. Dispersions characterisation

The blends with nanoparticles were analysed using Dynamic Light Scattering (DLS), also known as photon correlation spectroscopy or quasi-elastic light scattering, and Dark-field particle tracking system.

DLS measurements were performed using a Zetasizer Nano ZS (Malvern, UK). DLS is typically used to determine the size distribution profile of small particles in a suspension. As a representative result, the method gives the intensity [in %] as a function of particles sizes [nm].

Dark-field particle tracking system was developed at AC2T research GmbH, Austria [20]. The method utilizes dark field video microscopy for tracking and sizing plasmonic nanoparticles freely diffusing in a 10 μ m thin lubricant film confined between two glass substrates. By this method, all particles in the liquid film can be visualised since the whole sample fluid volume is illuminated. In this research we have used a particles visualization with dark-field microscopy recorded at 10 \times /0.3 objective. The equipment used in dark field configuration was an Axiotron microscope (Zeiss, Germany) with an additional magnification changer (1.25 \times to 2.5 \times), long working distance objectives (10 \times /0.3, 50 \times /0.45), and a D5100 camera (Nikon, Japan) using a resolution of 1920 \times 1080 at 25 fps. A 532 nm CW laser (Optotronics, USA) with a beam diameter of 1.5 mm and power of 20 mW was mounted at an angle of 20 $^\circ$ to the microscope stage. The focus was located at the middle of the 10 μ m thick film, and particles appeared as diffraction-limited spots (airy discs) of several micro-meters in diameter.

2.3. Tribological test set up

2.3.1. SRV[®] reciprocating sliding tribotests

The ball-on-disc tests were performed using a SRV[®] tribometer (Optimol Instruments Prüftechnik GmbH, Germany), where a 10 mm diameter steel ball was loaded and reciprocated against a stationary steel disc lubricated by a lubricant solution under boundary lubricated, pure sliding condition (Fig. 2a). The oscillation frequency was 10 Hz and the stroke 1.5 mm, which gives an average sliding speed of 0.04 m/s. The normal load was set to 25 N, which corresponded to an initial

mean contact pressure of 0.9 GPa. This simulates milder contact conditions, as those found in automotive engines (e.g. cam/tappet and ring/liner). All tests were conducted for 2 h at 40 $^\circ$ C. The test parameters are listed in the table seen in Fig. 2c.

2.3.2. Brugger tribotests

The Brugger-test is a standardized method [21] for determining the lubrication ability of additivated oils. The Brugger test is known to promote reaction of active additives, but it is less sensitive to the adsorptive agents. According to the Norm: DIN 51347-1 and 2, the Brugger-test creates a wear scar under friction conditions in the contact zone between a friction ring ($\varnothing=25$ mm) and a test cylinder ($\varnothing=18$ mm) (Fig. 2b). In the Brugger apparatus, the test cylinder rotates with a defined normal force and frequency on a counter friction ring. The lubricant to be investigated is distributed on the contact surface of the friction ring and after 30 s of incubation, the test cylinder is pressed to the friction cylinder using a defined test load of 400 N. This results in a mean contact pressure of 1.4 GPa and a maximum contact pressure of 2.11 GPa. The spindle of the Brugger lubrication tester imparts a relative velocity of 75 m/min during the test. After 30 s of test time, the worn area the test cylinder is measured and the so-called Brugger-value is evaluated as the ratio between the normal load and the worn area. The tests parameters are summarised in Fig. 2c.

2.4. Surface analyses

The tested specimens were rinsed in petroleum ether after the tribological tests. Afterwards, the wear tracks were examined by using a series of surface characterisation instruments including optical interferometer, scanning electron microscopy (SEM) with energy dispersive x-ray spectroscopy (EDX) and x-ray photoelectron spectroscopy (XPS).

2.4.1. Surface topography

Surface topography of the tested samples was evaluated using a Leica DCM 3D – combining interferometric and confocal microscopy (Leica, Japan). Surface roughness was measured before and after the tests according to ISO 4287. The Leica Map Premium 0.2.0190 software was used for wear volume analysis. The wear volume analysis method calculates the volume between the worn surface and a reference plane. The reference plane was set as the average height of the unworn area outside the wear track. The wear volume was calculated for the whole wear track and only the area under the reference plane was considered. Then, the removed wear volumes were normalised into wear coefficients (K) according to the Archard's equation:

$$K = \frac{V}{F \times S}$$

where, V is the remove wear volume (m³), F is the normal load (N), and S is the sliding distance (m).

In addition, wear tracks on the pins and discs were visually inspected using an optical microscope.

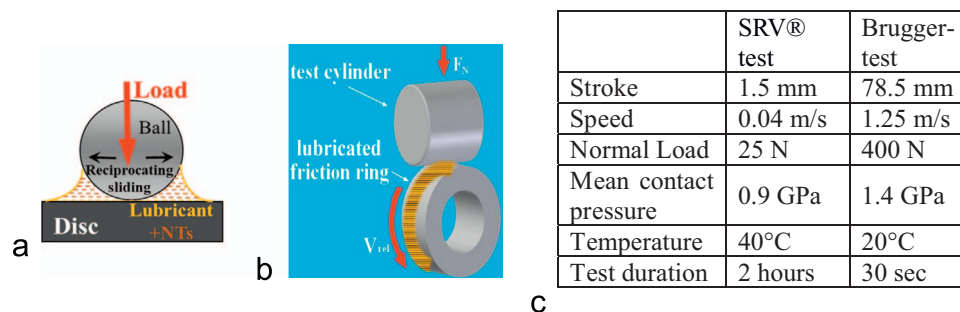


Fig. 2. Schematic of the experimental set-up a) SRV, b) Brugger, c) summary of the testing parameters of both tribotests.

2.4.2. Scanning electron microscopy

The SEM micrographs were obtained using a ZEISS SIGMA HD VP device. It is equipped with a Schottky field emission gun (FEG) for optimal spatial resolution (about 1 nm theoretically). The instrument can be used in high vacuum mode (HV), and in variable pressure low-vacuum mode (VP). This makes it possible to study samples in pressures up to 133 Pa. The microscope is equipped with a TEAM OCTANE PLUS Version. 4.3 from EDAX Energy Dispersive X-ray (EDX) system for chemical analysis. The spectra were collected at 10 and 20 keV and the acquisition time was 60 s.

2.4.3. Focus ion beam

Focus Ion Beam cuts were performed using FIB QUANTA 200 3D from FEI. The accelerating voltage for FIB was 30 kV, the currents used for milling were 7 nA; 0,5 nA; 0,1 nA, and the current used for imaging was 10 pA. The final size of the FIB cut was 10 μm deep and 30 μm width. Prior to the ion milling process, Pt-protective layer was deposited on top of the surface using a current of 0,3 nA, which resulted in a thickness of 1,5 μm .

2.4.4. X-ray photoelectron spectroscopy

XPS measurements of the tribofilms were performed using a Thermo Fisher Scientific Theta Probe (East Grinstead, UK), equipped with a monochromatic Al K α X-ray source ($h\nu=1486.6$ eV) and an Ar⁺ ion gun.

Prior to the XPS analysis, the tested samples were ultrasonically cleaned in petroleum ether (HPLC grade), for 10 min. After being transferred inside the XPS chamber, adventitious carbon was removed from the samples by a sputtering using 3 kV and 1 μA sputter current for 10 s. The cleaned area was approximately 3 \times 3 mm, which resulted in a surface removal of about 0.2 nm. The wear tracks generated under reciprocated sliding were analysed using a spot size of 100 μm . For the wear tracks obtained using the Brugger tests, the spot size was adjusted to 400 μm . The elemental composition of the respective surfaces was elucidated by survey scans with a resolution of 200 eV. The detailed spectra of the particular elements were acquired with a resolution of 30 eV.

The resulting binding energies were referenced to the adventitious carbon at a binding energy of 284.6 eV. All the acquired spectra were processed with the Average Data System software 5.962 (Thermo Fisher Scientific, East Grinstead, UK), using Gaussian/Lorentzian peak fitting for the high resolution scans.

3. Results

3.1. Dispersions stability

The nanotubes size distribution and their dispersion stability in the lubricant blends were evaluated using dark field particle tracking method (DFT) and Dynamic Light Scattering (DLS). For this, NTs dispersions in the different lubricant mixtures were prepared as a 10 μm thin liquid film placed between two substrates and visualised using DFT. Subsequently, the particle size distribution on the same mixtures was measured using DLS.

The results of the DFT and DLS measurements show the role of each additive on the dispersion stability of NTs in the oil blends. In particular, it was observed that blends containing solely NTs or NTs accompanied by ZDDP had a strong agglomeration of NT particles in the fluid as shown in the example of Fig. 3a. According to DFT (also proven by optical microscopy measurements) the clusters of NTs can reach sizes ranging from 20 to 50 μm . DLS is not able to capture this cluster size since it is out of its measuring range and wrongly determines that the particle sizes are approximately 3 μm .

After introducing either the EP additive, dispersant or detergent the distribution of NTs within the mixtures was homogenous as in Fig. 3b. Particles sizes according to DLS measurements were always below

1 μm for all well-dispersed lubricant mixtures.

Apparently among the additives used in fully formulated oils, extreme pressure, detergents and dispersants are able to interact with NTs in order to keep all suspended particles apart and well dispersed. The additives used in our studies were provided by a major additive company, and are thus believed to be representative of those currently used in common automotive lubricants.

3.2. Friction performance

In order to better understand the effect of additives on the tribological performance of nanotubes, reciprocating sliding tests were carried out using the prepared lubricant mixtures. The results are presented in a form of frictional scan as a function of time (Fig. 4). It is important to note that the error bars presented on the frictional curves represent the average of three repetitions, and it can be stated that reproducibility of the results was very good for all test conditions, except for PAO+EP additives (Fig. 4b). As expected and reported previously by many researches [2,9,13], the lowest coefficient of friction (COF) of 0.05 was reached for the base oil mixed only with NTs (Fig. 4a). In order to illustrate their tremendous friction reducing capacity, the results obtained for reference PAO oil, PAO+AW, PAO+AW+NTs and a sequence of PAO+ZDDP followed by PAO+NTs are shown together in Fig. 4a. The presence of AW additive does not influence the base oil performance in terms of friction, while the addition of NTs to this blend reduces the COF down to 0.10. A reduction to lower values (\sim 0.05) requires the presence of a well established ZDDP tribofilm, as shown with a test pre-rubbed using ZDDP and afterwards adding the NTs. The presence of EP additives results in a worse performance, when compared to PAO, as shown in Fig. 4b. However, the addition of NTs to this blend is able to improve and stabilize the COF to a value of 0.11. The reason for the poor performance of PAO+EP could be due to the too mild conditions achieved in the SRV tribocontact, insufficient to activate the additive. On other hand EP additive is not expected to reduce COF, since it mainly protects the surface from wear. Fig. 4c shows slightly higher COF for base oil additivated with detergent. Nonetheless, NTs fulfilled their function as friction modifiers and their addition to the blend resulted in a reduction of the COF to 0.10. The worst performance of NTs was observed for the mixture of NTs accompanied with dispersant. As shown in Fig. 4d, only a scant improvement can be achieved compared to PAO+disp blend. This antagonistic interaction between dispersant and MoS₂ nanoparticles was also reported by Rabaso et al. [10].

The frictional disc surfaces after the reciprocating sliding tests were analysed using SEM/EDX in order to reveal the interaction mechanisms between NTs and additives under the tested conditions. The results are shown in Fig. 5. By observing the SEM morphologies of the both wear tracks (with and without NTs) it seems that there was almost no surface damage occurring in this central area where the micrographs were taken. The discs after the tests were rinsed with petroleum ether. However the nanotubes-based film was not removed, as EDX shows the clear presence of Mo/S peak. Thus, the EDX analysis confirmed the presence of thin (not visible) tribofilm at the surface deriving from the MoS₂ nanotubes. The blends containing only PAO with additive reveal the presence of the elements characteristic for the type of tribofilms formed, for instance Zn, P for ZDDP and Ca, for detergent. When adding NTs to the model mixtures, the presence of Mo/S was always observed, indicating for some of the additives the presence of a tribofilm derived from the NTs. In case of EP and detergent, the presence of a Mo/S peak may also arise from the additive and the tribofilm analyses requires the use of other techniques such as XPS.

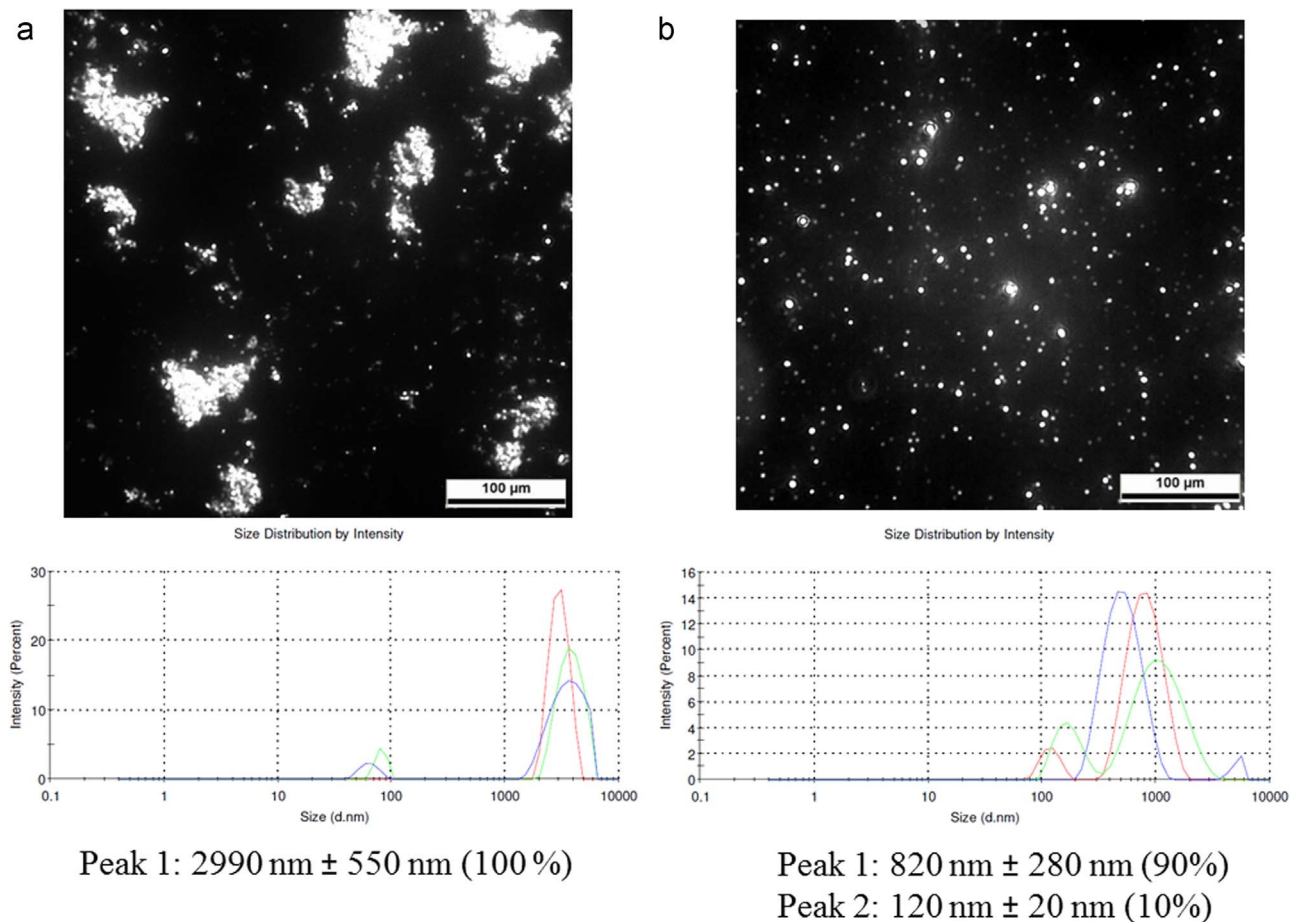


Fig. 3. Dark-field microscope image followed by Dynamic Light Scattering Intensity graph and numerical results of particles size distribution in lubricant blend of a) PAO+NTs and b) PAO+disp+NTs.

3.3. Interaction between NTs and additives under extreme pressure

A second experimental setup to evaluate the synergistic effects between nanotubes and conventional additives under extreme pressure conditions was the Brugger tribotest. The results in terms of load-carrying capacity (LCC) are shown as column graphs in Fig. 6. The color bars denote the value of the load carrying capacity and these are extended by error bars shown in red color. Clearly, the reproducibility of the experiments was good, in particular for low load-carrying capacities. The Brugger tests reveal a clear improvement of the load-carrying capacity for all lubricants containing NTs, independently from the additive present in the fluid. The only exception was for extreme pressure additives, where the performance of EP was already excellent and was even further improved by the presence of the NTs. Under the presence of dispersant and detergent, NTs are very effective, even the results show a slightly higher standard deviation. The exclusive use of NTs in the base oil (without further additives) leads to the second best performance after EP+NTs, in terms of load-carrying capacity.

Reference tests with PAO 4 show a very low load carrying capacity, and the wear tracks as shown in Fig. 7a reveal the presence of substantial wear debris inside and around the wear track. For all the tests with lubricant mixtures containing NTs (Fig. 7b–f) no wear debris were spotted, only a very homogenous wear track with a trace of material pushed by plastic deformation from inside to outside the track along the test direction. It can be concluded from the presented images that material removal by wear is reduced, when NTs are in the contact due to the low shear provided by the MoS₂ nanotubes and inconspicuous wear debris formed in the contact.

SEM and EDX analysis on the Brugger cylinders after the tests are shown in Fig. 8. After test with PAO+NTs (Fig. 8a) and PAO+AW+NTs (Fig. 8b) dark zones were spotted on the wear tracks. EDX proved that those dark fields are rich in Molybdenum, while in the bright surface around the wear track the concentration of this element is rather poor. The wear tracks after the tests with PAO+EP+NTs (Fig. 8c), PAO+det+NTs (Fig. 8d) and PAO+disp+NTs (Fig. 8e) shows Mo rich dark spots instead of zones. This results can be nicely correlated with dispersity of the NTs in the lubricant mixtures, as observed by DFT and DLS (Fig. 3). For the PAO+NTs and PAO+AW+NTs clusters of NTs were detected – this explains larger zones rich in Mo on the wear tracks (Fig. 8a and b). In case of lubricants blended with EP, detergent and dispersants, the NTs were distributed homogenously – that is why only smaller spots are present on the Brugger's wear track surfaces. Although very small spots rich in Mo were found scattered across the surface, these were sufficient to achieve a very high load carrying capacity according to Brugger, comparable or even superior to the one achieved by the much larger Mo rich areas of PAO+AW and PAO+AW+NTs (Fig. 6).

3.4. Role of contact conditions on friction, wear and tribofilm formation

The frictional surfaces after reciprocating sliding and Brugger tests were analysed with Leica 3D interferometric and confocal microscopy, as described in Section 2.3. Based on these data, the removed wear volume was measured by subtracting the measured topography from a reference ideally flat surface. The wear volumes were normalised by load and sliding distance in order to calculate the Archard wear

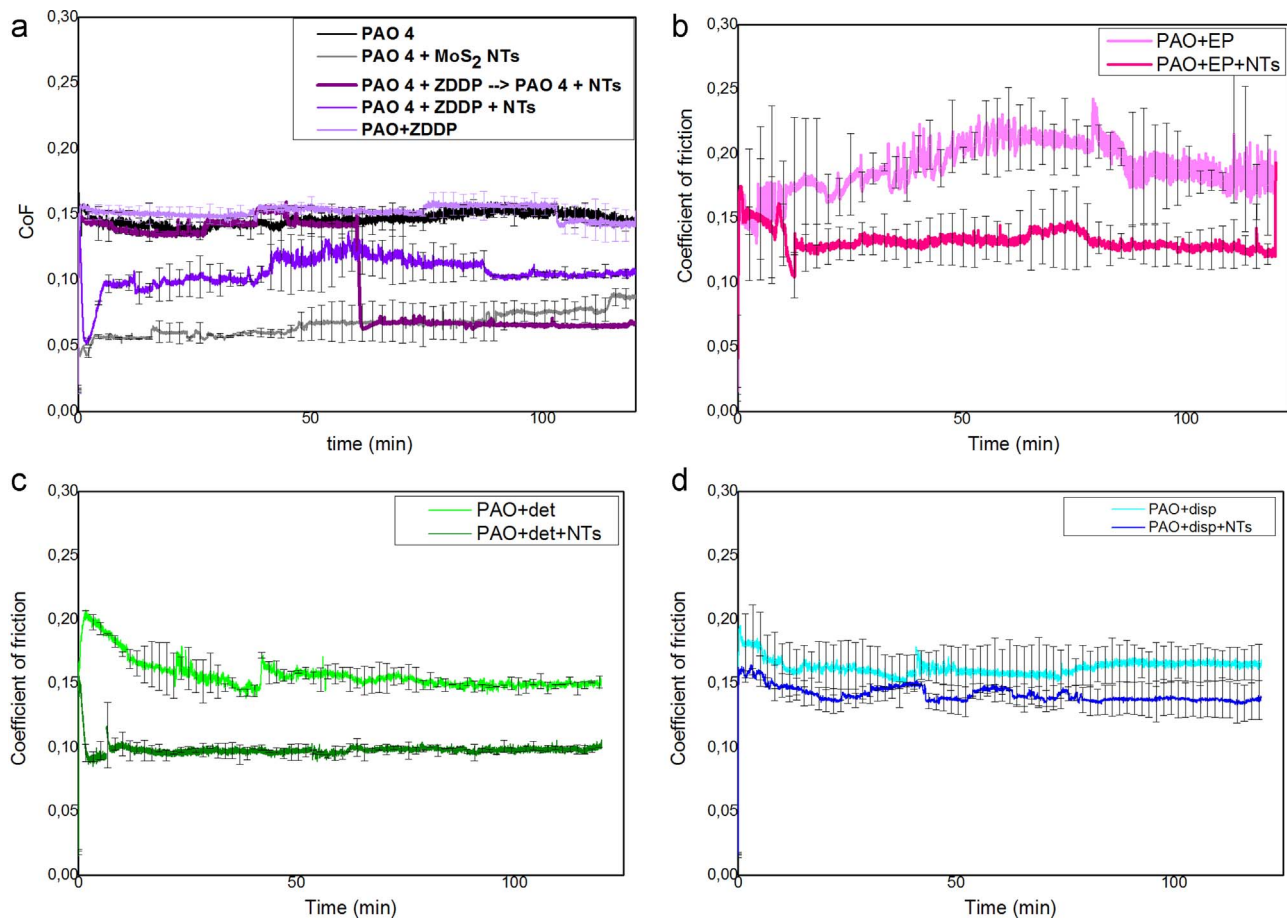


Fig. 4. SRV tests results represented with friction curve including error bars distribution over the curve for following groups of additives a) reference PAO oil, PAO+NTs, PAO+AW and PAO+AW+NTs; b) PAO+EP and PAO+EP+NTs; c) PAO+det and PAO+det+NTs; d) PAO+disp and PAO+disp+NTs.

coefficient for each tribotest performed within this work. The summary of all Archard wear coefficients for reciprocating sliding and Brugger test is shown in Fig. 9. Archard wear coefficients after Brugger tests are about four orders of magnitude higher when compared to the reciprocating sliding tests, since the contact conditions are different in both cases. The wear coefficient in the reference tests performed with PAO is the highest. The addition of NTs in the base oil reduces wear by at least 80% in the SRV and over 90% in the Brugger tests. However further addition of conventional additives does not improve the results in such a large amount anymore. It is also remarkable that under reciprocating sliding, even the addition of additives to the lubricant mixture containing base oil with nanotubes is not able to maintain the reduced value of the coefficient of friction achieved with only nanotubes, in terms of wear, all this mixtures provide a significant improvement.

In order to analyse in detail the tribofilm formed by AW ZDDP and NTs on steel shown previously in Fig. 5b, the surface was further analysed on SEM/EDX by making a transversal cut using FIB. The chemical analysis with EDX taken on the tribofilm area confirms the presence of Zn and Mo, as presented in Table 2. These results indicate that greatest portion of the tribofilm consist of ZDDP-derived tribolayer, while MoS₂-derived products are found to be trapped and/or exfoliated within the bulk layer of the tribofilm. Similar tribofilm formation has been reported earlier by Tomala et al. [1] on a steel surface without the presence of ZDDP additive (only NTs and PAO). This can be explained by progressive oxide/ZDDP film formation followed by gradual exfoliation and transfer of molecular sheets onto the asperities of the reciprocating surfaces and it is with agreement with the literature [22]. This explains the presence of small amounts of molybdenum or sulphur embedded in the ZDDP layer.

A synergistic effect in terms of friction was also observed on the SRV tests between the selected overbased Ca-sulfonate dispersant and the NT. In this case, the XPS analyses reveal mainly the presence of calcium on the tribofilm, as expected by the observations done in Fig. 5f using SEM/EDX. Besides the strong calcium signal, the presence of molybdenum could be also confirmed in agreement with the EDX analyses indicating that NT can still exfoliate on top of the calcium and provide friction reduction. Small amounts of iron sulphide could be also identify, which indicate that either the sulphur of the additive or the nanotubes is able to react with the Fe surface to form small amounts of sulphide compounds. In any case, the amount was much lower than in the presence of EP additives.

In case of EP with NT, the SRV tests reveal that NT are able to slightly improve the friction performance of the lubricant mixture. XPS analyses show the presence of clear MoS₂ peaks on the Mo spectra (Fig. 10a), which reveal that under the presence of EP additives, MoS₂ are still able to exfoliate on top of the iron surface during the tribological contact. The clear presence of iron sulphides could be also identified and with higher intensity than for det+NT. Even though a small amount may be due to reaction of the NT with the Fe surface, this result is a hint that the sulfurized olefin is still able to react and becomes active during the tribotest, indicating a surface competition between EP and NT. Further evidence for the reaction of the EP additive is, that the binding energy of 161.3 eV detected for the sulphides is typical for metal sulphides and not for organic bound sulphide structures, which are in the region of about 163 eV binding energy. Under the lack of NT, the XPS analyses of the steel surface after the SRV tests using EP additive alone show a smaller total amount of sulphides, being all of them attributed to the formation of iron sulphides (Fig. 10b. S peak EP compared with EP+NT).

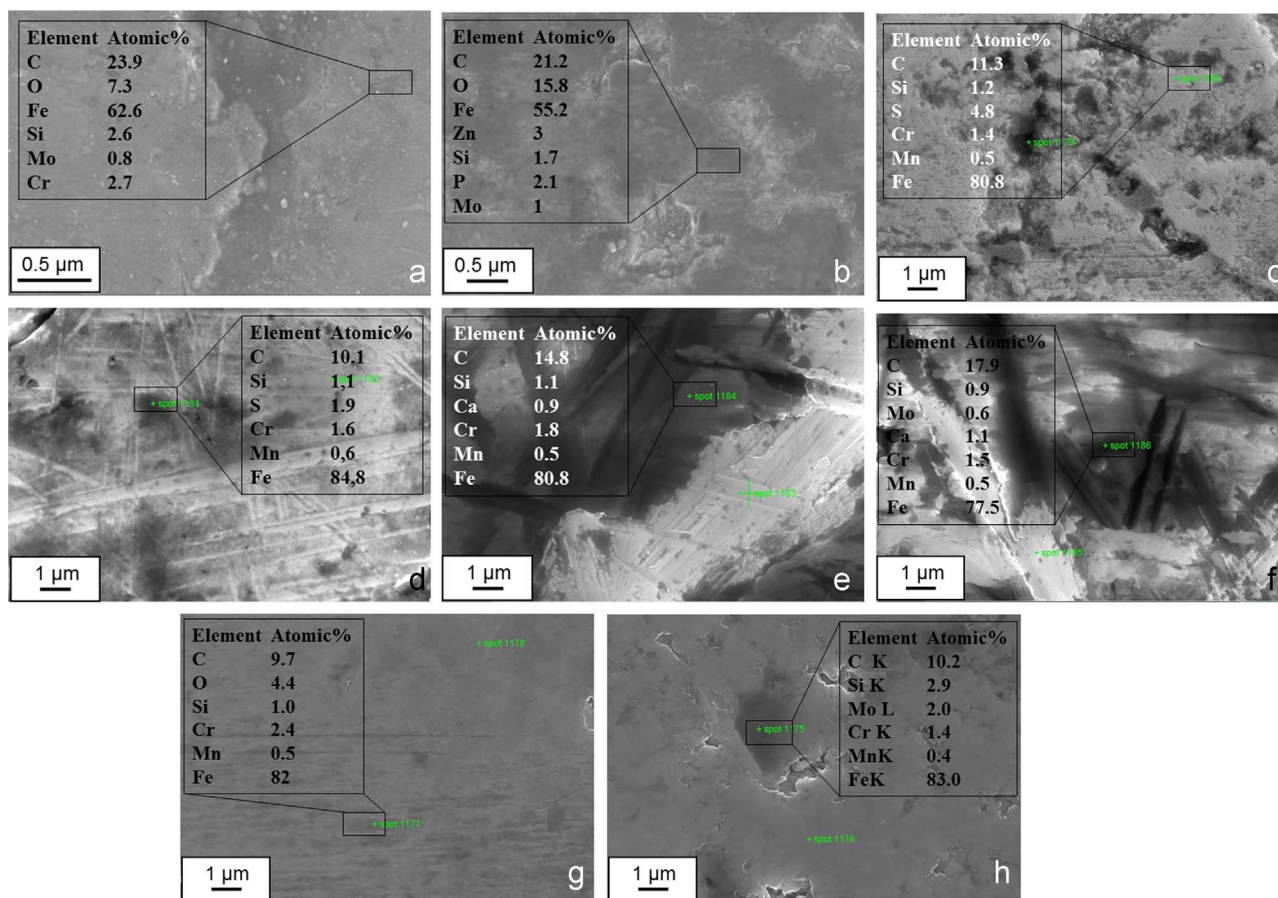


Fig. 5. SEM micrographs of a wear scar on SRV disc after the tests lubricated with a) PAO+NTs and b) PAO+AW+NTs., c) PAO+EP and d) PAO+EP+NTs; e) PAO+det and f) PAO+det+NTs; g) PAO+disp and h) PAO+disp+NTs.

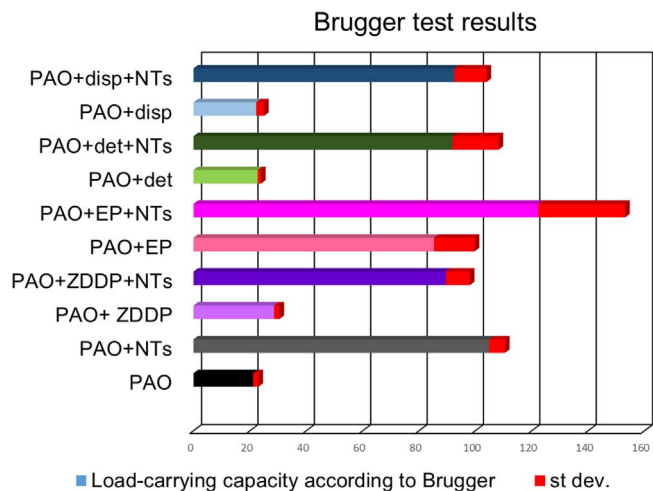


Fig. 6. Load carrying capacity results of Brugger tests for lubricants with additives and nanotubes.

Finally the presence of dispersants leads to an antagonistic synergy with NT. The XPS measurements highlight the lack of MoS₂ peaks on the Mo spectrum and reveals the presence of molybdenum oxides (Fig. 10a). Combined with the small presence of iron sulphides that could be detected and since the only source of S are the NT, the XPS measurements suggest the degradation of the MoS₂ NT during the tribological contact.

In contrast to the reciprocating sliding results, all additives were able to provide an excellent synergy with MoS₂ nanotubes in terms of load carrying capacity under the much more severe contact conditions

of the Brugger test. The reason for this improvement is uncovered by the XPS data. In all investigated cases, the results show a strong formation of iron sulphides in the wear scar. All spectra of the surfaces tested show a very similar peak as the one measured using exclusively EP additive (Fig. 11b). On the other hand the molybdenum spectra show the formation of molybdenum oxides, particularly when using dispersant and detergent (Fig. 11a). In all cases, the presence of molybdenum is very weak and in the form of oxides. An extreme case was for the blend containing EP+NT, where only very small amounts of Mo could be detected in the three investigated samples.

4. Discussion

The aim of this work was to characterize the tribological performance of MoS₂ nanotubes (NTs) in the presence of conventional additives. The group of anti-wear additives (AW) was represented by ZDDP (zinc dialkyl dithiophosphate), extreme-pressure additives (EP) by active sulphurized olefin 40%S, dispersants (disp) by succinimide and detergents (det) by overbased Ca-sulfonate. The presented results reveal synergistic and antagonistic effects in terms of friction, load carrying capacity, wear and tribofilm formation between NTs depending on the accompanying additive and the selected contact conditions.

The friction and wear performance under reciprocating sliding contact conditions were investigated using SRV friction tests in boundary lubrication regime, at 40 °C for 2 h using steel ball on disc configuration. A comparison of friction curves for additivated and non-additivated lubricants containing NTs shows the following highlights. In pure PAO, NTs are able to reduce the coefficient of friction by 55% compared to reference PAO oil. The coefficient of friction (CoF) is very stable and the reproducibility of the tests is also excellent, especially in

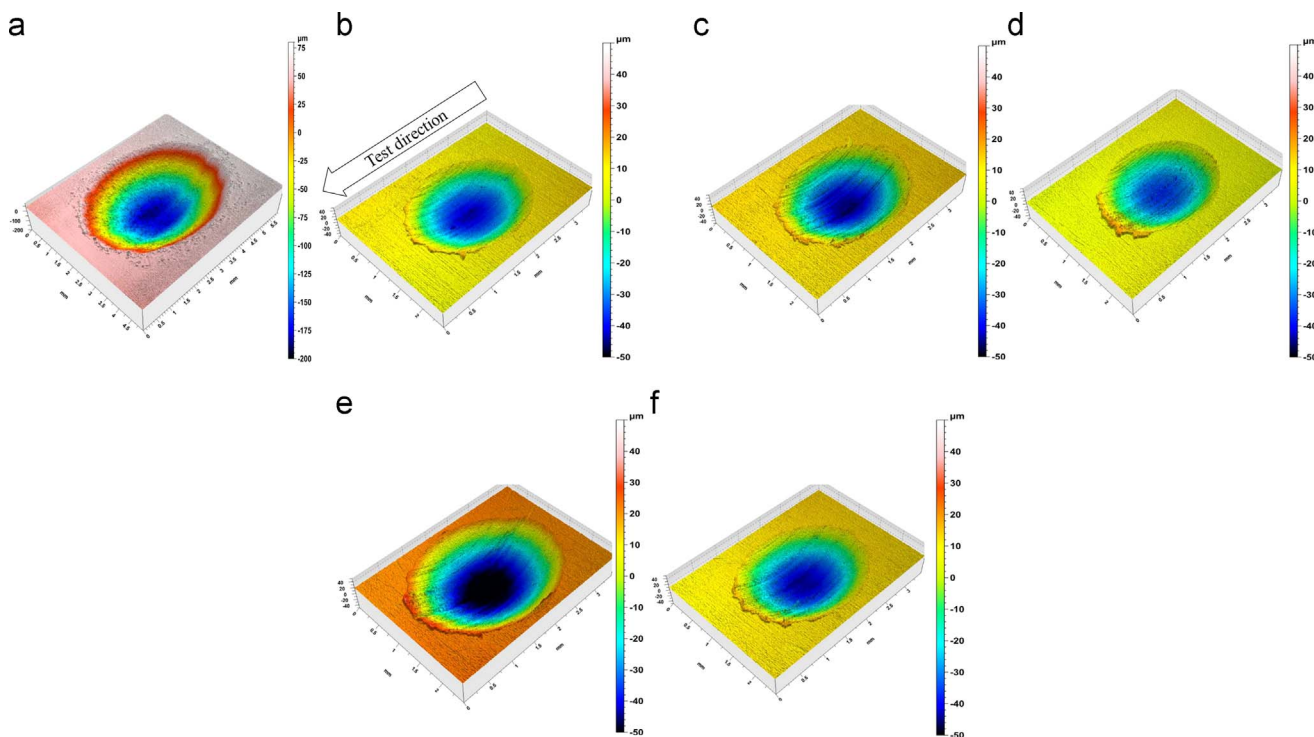


Fig. 7. 3D topography scans of the worn area after the Brugger tests for a) reference PAO oil b) PAO+NTs c) PAO+AW+NTs d) PAO+EP+NTs e) PAO+det+NTs f) PAO+disp+NTs. Note the different scale used in a) due to the larger dimensions of the wear scar.

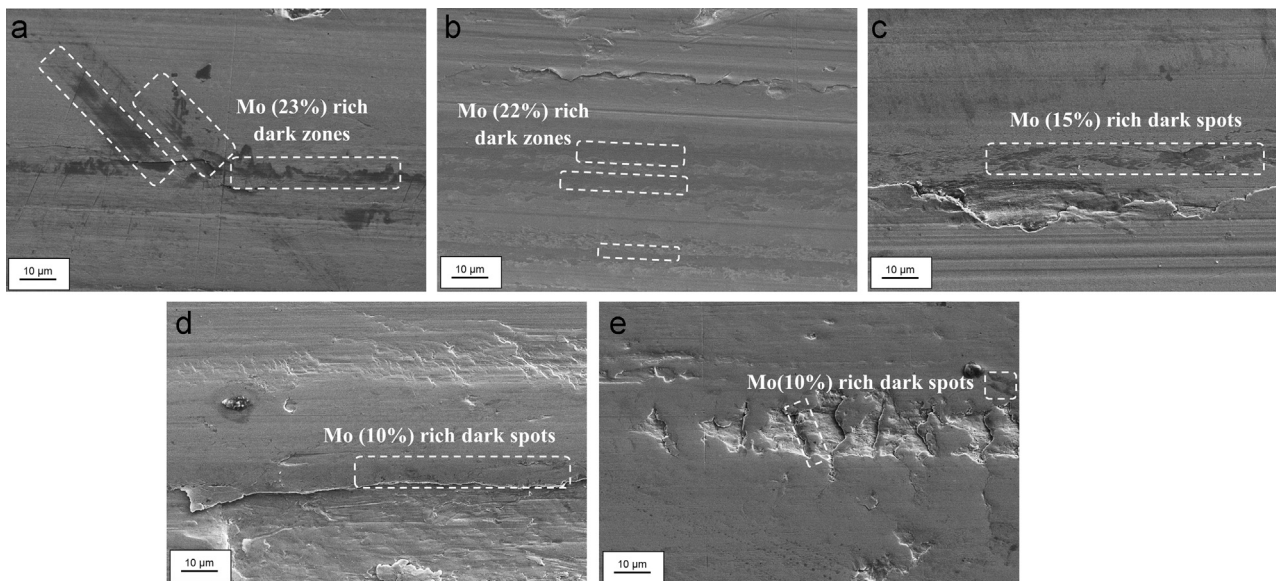


Fig. 8. SEM and EDX analysis of Brugger wear marks for a) PAO+NTs b) PAO+AW+NTs c) PAO+EP+NTs d) PAO+det+NTs e) PAO+disp+NTs.

the first hour. These results are very similar and can be directly compared to those obtained in the literature [1,11,13,23]. All tested groups of additives diminish the friction modifier effectiveness of NTs when they are present in the lubricant. AW and EP additives with NTs reduced the CoF by 30% compared to PAO+AW and PAO+EP, detergent with NTs reduced the CoF by 38% compared to PAO+det and had the most stable results of all tested blends. The NTs were almost completely ineffective in terms of friction reduction in the presence of dispersant: they reduced the averaged CoF by only 13%. This antagonistic effect of succinimide dispersant on MoS₂ nanoparticles was also reported by Rabaso et al. [10]. Although the NTs accompanied with additives showed different influence on the CoF, in terms of wear the Archard wear coefficient in SRV tests was very

similar in all mixtures containing NT. A maximum increase of wear was observed for samples tested with PAO+EP+NTs.

The tribological performance of NTs combined with additives can be explained in terms of tribofilm formation based on the results obtained with SEM-EDX and XPS. The frictional surfaces after SRV tests showed under SEM-EDX the presence of a thin (not visible) Mo-containing tribofilm at the surface, obviously deriving from MoS₂ nanotubes. The synergistic effect between NTs and ZDDP could also be highlighted within the present work and is in agreement with results reported in literature [1,13]. A FIB cross section and subsequent EDX chemical analysis of the tribofilm formed by PAO+AW+NTs on steel surface showed the presence of Zn and Mo. In previous works using higher resolution TEM analyses [1,13], the synergy between NTs and

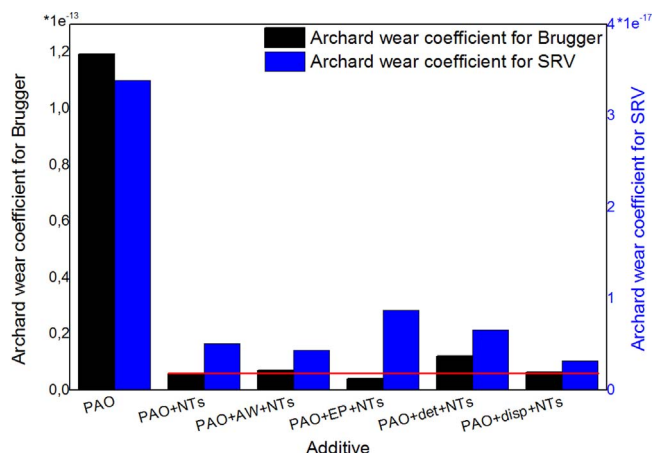


Fig. 9. Archard's wear coefficient calculated for wear tracks on Bruggen cylinders and SRV discs.

Table 2

EDX analysis performed on a FIB cross-section of the tribofilm after the SRV tests lubricated with PAO+AW+NTs.

C K	29.3
O K	14.3
Fe L	22.8
Zn L	5.7
Ga L	9.3
Pt M	15.8
Mo L/S K	2.8

ZDDP was found to be related to the exfoliation of transition metal dichalcogenide nanoparticles on top of a well-formed ZDDP tribofilm. In case of [13] this occurs by supporting ZDDP tribofilm formation by a higher testing temperature, whereas in [1] and in our case, this is achieved by pre-rubbing with ZDDP additive. When using a PAO +ZDDP+NT mixture at 40 °C as in the present work, the synergistic effect is not so pronounced, probably due to the lack of a well-established ZDDP tribofilm. This leads to partial embedment of the nanotubes on the ZDDP tribofilm, instead on exfoliation on top of it.

A synergistic effect has been also observed within the present work between NTs and overbased Ca-sulfonate detergent. In this case, the SEM-EDX analyses show the presence of a very similar Ca-based tribofilm with or without the presence of NTs, with the difference that Mo signal could be detected in the former case. This indicates that the NTs are able to exfoliate under the presence of the formed Ca-based

tribofilm and provide a significant friction and wear reduction. On the other hand, a rather small synergy could be identified between NTs and sulfurized olefin EP additives. The presence of a strong MoS₂ XPS signal combined with the identification of iron sulphides suggests that even though the NTs are able to exfoliate under the presence of EP, the MoS₂ lamellas will have either to compete with the EP additives for the surface or to directly exfoliate over formed iron sulphide tribofilm. This results in a slight decrease in friction, but to a much lower extent when compared to the improvement observed with either ZDDP or overbased Ca-sulfonate. Despite the formation of iron sulphides during rubbing, which are known to have excellent extreme pressure properties and increase the load-carrying capacity, the wear coefficient was the highest one measured on the SRV tests of all mixtures containing NTs. The highest antagonistic effect was found between NTs and succinimide dispersants. According to literature, the reason for the lack of friction reduction under reciprocating sliding is not that dispersants prevent transition metal dichalcogenide nanoparticles to enter the contact and be trapped by the counteracting bodies nor that do they avoid the exfoliation of the TMD lamellas. Instead, the reason is the suppression of the adhesion of the generated TMD lamellas to the surfaces in order to enable low friction by the easy shearing of TMD lamellas [10]. In our results, this antagonistic effect was clearly manifested in the friction plots. However, contrary to previous observations, the XPS data revealed the formation of a tribofilm formed by small amounts of molybdenum oxide and iron sulphides, indicating a possible decomposition of the nanotubes during the tribological contact.

The synergy between MoS₂ nanotubes (NTs) and the selected additives was investigated under severe contact conditions using a Bruggen test setup. The load carrying capacity measurements were performed under mixed lubrication regime for 30 s at room temperature using cylinder on ring configuration. Similar to SRV test, the lubricant mixture containing only PAO+NTs had an excellent load carrying capacity, increasing the load carrying capacity by 85% compared to reference PAO oil. This mixture could be only outperformed by the mixture containing EP+NTs. The presence of other additives slightly diminish the effectiveness of NTs, but to a much lesser extent when compared to SRV tests. Contrary to the SRV tests, the NTs in the presence of dispersant have the same effectivity as in the presence of detergent and AW additive. Otherwise all additives alone had a rather poor performance on the Bruggen test except the EP additive. Under PAO+EP, the load carrying capacity increased by 70% compare to the reference PAO oil, and further addition of NTs to this blend improve the results by 50%. Also the wear track and Archard wear coefficient are minimal for mixtures containing EP additives. Generally, it can be summarised that the material removal is strongly reduced when NTs are in the contact either accompanied or not with

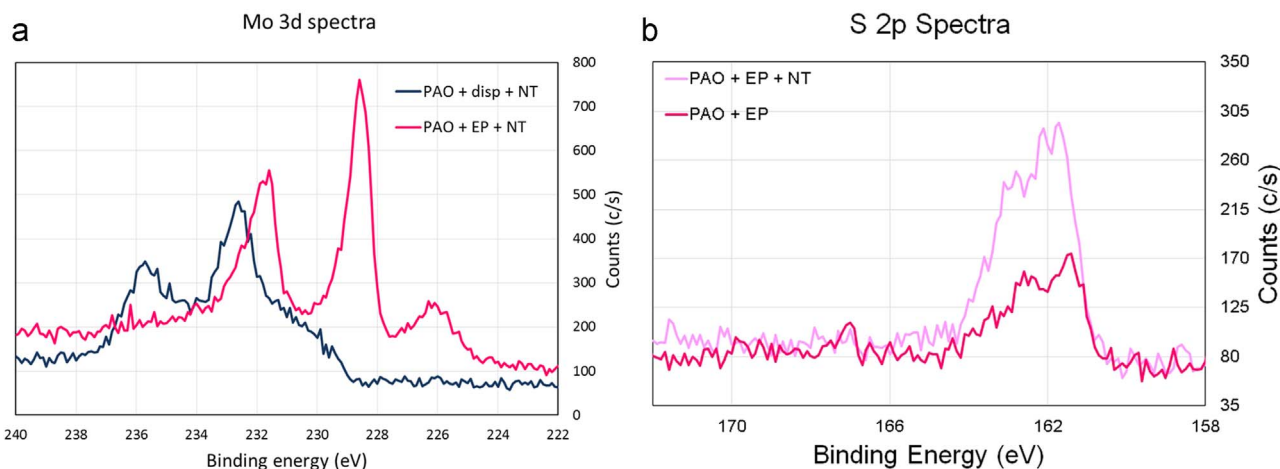


Fig. 10. Mo 3d spectra tribolayer generated in SRV test by the PAO+disp+NT and PAO+EP+NT blends (a) S2p spectra of the tribolayer generated in SRV test by the PAO+EP+NT and PAO+EP blends (b).

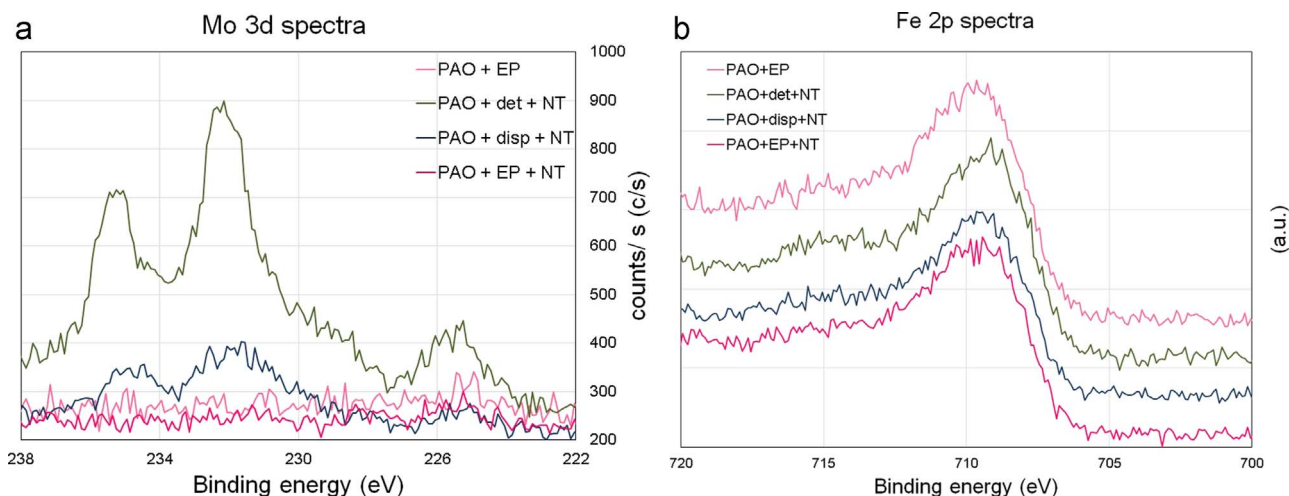


Fig. 11. Comparison of the Mo3d spectra (a) and Fe 2p spectra (b) measured in the wear track after the Brugger test.

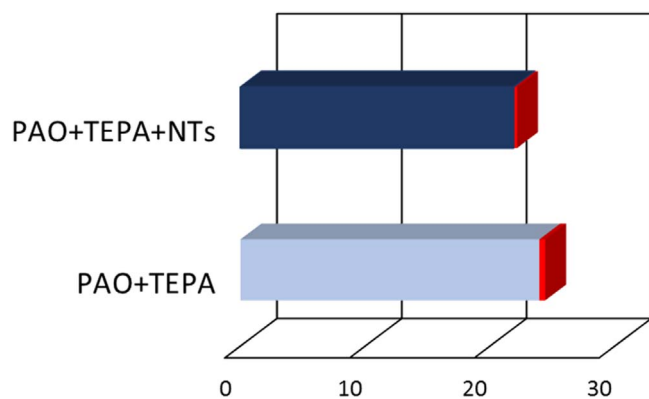


Fig. 12. Load carrying capacity results of Brugger tests for TEPA.

the selected additives. In order to try to find a counterexample, the authors repeated the tribological tests using a combination of Tetraethylenepentamine (TEPA) dispersant and NTs. The results show that under the presence of TEPA, an antagonistic effect can be observed with both, SRV tests and Brugger (Fig. 12). This additional test is an indication that even under the presence of most additives the LCC will be improved in combination with NTs, this statement is not always valid and special precaution is required for prospective formulations.

The reason for the improvement in load carrying capacity under the presence of most of the additives could be disclosed based on the analyses of the wear scars. Surfaces after the Brugger tribotests analysed using SEM-EDX clearly showed visible dark zones and spots rich in molybdenum and sulphur, indicating the local presence of MoS₂. Interestingly, it was noticed a correlation between the dispersant properties of the additives mixed with the NTs and the distribution of Mo spots on the wear scars. For instance, in case of PAO+NTs and PAO+AW+NTs clusters of NTs were detected in the mixtures and this explains large zones rich in Mo and S on the wear tracks after Brugger. In case of lubricants blend with EP, detergent and dispersants, the NTs were distributed uniformly and that is why only small Mo and S-rich spots were detected on the wear track surfaces. The load carrying capacity according to Brugger for all blends where NTs were present was very high, independently on the amount of dark spots and Mo-rich zones sizes.

The XPS data show that under the severe contact conditions undergone during the Brugger test, all tested mixtures containing NTs revealed the presence of a tribofilm formed by iron sulphides and molybdenum oxides emphasising the ability of transition metal dichalcogenides (TMD) nanotubes to react with iron surfaces. The formation

of these reaction products was already observed in the literature using other TMD nanoparticles [24–27]. The most recent of these works comprises the investigation of two morphologies of WS₂ (2H flat sheets and inorganic fullerene-like IF nanoparticles) and IF WSe₂ nanoparticles, which were mixed with PAO6 base oil. The test conditions were severe in terms of temperature 100 °C and contact pressure (1 GPa). In all cases, a reaction of the nanoparticles with the substrate leading to the formation of iron sulphides/selenides, elemental tungsten and tungsten oxides could be measured by XPS. These results evidenced the reaction of the nanoparticles with the iron present on the surface according to the chemical reaction (1) and are in consonance with the present results. However, under extreme pressure conditions, the temperatures required at the asperity contacts for the reaction to take place would be a function of pressure and temperature and could occur at temperatures lower than 720 °C. The novel information obtained within our work is that this reaction of TMD nanoparticles under extreme contact conditions occurs independently of the presence of the selected oil additives in the mixture. The reaction with iron leads to the formation of tribofilms with superb antiwear properties due to the combined presence of iron sulphides and molybdenum disulphide, as highlighted in [25–27]. Contrary to their observation that the formation of these tribofilms require high temperatures, in our case we showed that tribofilm containing iron sulphides can be formed under severe contact conditions at room temperature.

5. Conclusions

- MoS₂ nanotubes in unadditivated PAO oil provide the lowest value of friction in reciprocating sliding and the second highest load carrying capacity in the Brugger tests.
- MoS₂ nanotubes in combination with ZDDP are able to replicate the low friction values obtained with MoS₂ nanotubes alone, provided that a well-formed ZDDP is present on the wear track. The synergistic effect is attributed to the exfoliation of MoS₂ nanotubes on top of the ZDDP tribofilm, enabling easy shear between MoS₂ lamellas and thus reducing friction.
- Overbased Ca-sulfonate detergent and sulfurized olefin EP additive diminish the effectiveness of nanotubes in reducing friction, but a significant improvement can still be noticed. The detergent forms a Ca-based tribofilm, which does not prevent exfoliation of the MoS₂ nanotubes on it. On the other hand, the competition between highly reactive EP additive and MoS₂ nanotubes together with the pre-formation of an iron sulphide tribofilm prevents the MoS₂ nanotubes for providing low friction.
- MoS₂ nanotubes are not able to reduce friction under boundary conditions in the presence of succinimide dispersants, which is

attributed to the formation and presence of iron sulphides and molybdenum oxide on the wear track due to the degradation of the nanotubes.

- Under reciprocating sliding, MoS₂ nanotubes show superb anti-wear properties in combination with any of the selected additives. The mechanisms of tribofilm formation, however, are different depending on the accompanying additive.
- In the Brugger tests, MoS₂ nanotubes are able to boost the load carrying capacity under the presence of most of the selected oil additives. Without nanotubes, only the combination of PAO with EP additive is effective.
- The increase in load carrying capacity in the Brugger tests is attributed to the reaction of the MoS₂ nanotubes with the iron surface forming anti-wear tribofilms. The presence of dark spots corresponding to MoS₂ patches is also visible independently of the additive used, but their size and morphology could be correlated with the dispersant properties of the additive.

Acknowledgements

This work was funded by the Austrian COMET Programme (Project K2 XTribology. No. 849109) and carried out at the “Excellence Centre of Tribology”.

References

- [1] Tomala A, Vengudusamy B, Rodríguez Ripoll M, Naveira Suarez A, Remškar M, Rosentsveig R. Interaction between selected MoS₂ nanoparticles and ZDDP tribofilms. *Tribol Lett* 2015;59:1–18. <http://dx.doi.org/10.1007/s11249-015-0552-z>.
- [2] Kalin M, Kogovšek J, Kovač J, Remškar M. The formation of tribofilms of MoS₂ nanotubes on steel and DLC-coated surfaces. *Tribol Lett* 2014;55:381–91. <http://dx.doi.org/10.1007/s11249-014-0366-4>.
- [3] Shahnazar S, Bagheri S, Abd Hamid SB. Enhancing lubricant properties by nanoparticle additives. *Int J Hydrogen Energy* 2016;41:3153–70. <http://dx.doi.org/10.1016/j.ijhydene.2015.12.040>.
- [4] Remškar M, Viršek M, Mrzel A. The MoS₂ nanotube hybrids. *Appl Phys Lett* 2009;95:2–4. <http://dx.doi.org/10.1063/1.3240892>.
- [5] Remškar M, Mrzel A, Viršek M, Jesih A. Inorganic nanotubes as nanoreactors: the first MoS₂ nanopods. *Adv Mater* 2007;19:4276–8. <http://dx.doi.org/10.1002/adma.200701784>.
- [6] Tenne R, Margulis L, Genut M, Hodes G. Polyhedral and cylindrical structures of tungsten disulphide. *Nature* 1992;360:444–6.
- [7] Spikes H. Low- and zero-sulphated ash, phosphorus and sulphur anti-wear additives for engine oils. *Lubr Sci* 2008;20:103–36. <http://dx.doi.org/10.1002/ls.57>.
- [8] Bakunin VN, Suslov AYY, Kuzmina GN, Parenago OP, Topchiev AV. Synthesis and application of inorganic nanoparticles as lubricant components—a review. *J Nanopart Res* 2004;6:273–84. <http://dx.doi.org/10.1023/B:NANO.0000034720.79452.e3>.
- [9] Rabaso P, Ville F, Dassenoy F, Diaby M, Afanasiev P, Cavoret J, et al. Boundary lubrication: influence of the size and structure of inorganic fullerene-like MoS₂ nanoparticles on friction and wear reduction. *Wear* 2014;320:161–78. <http://dx.doi.org/10.1016/j.wear.2014.09.001>.
- [10] Rabaso P, Dassenoy F, Ville F, Diaby M, Vacher B, Le Mogne T, et al. An investigation on the reduced ability of IF-MoS₂ nanoparticles to reduce friction and wear in the presence of dispersants. *Tribol Lett* 2014;55:503–16. <http://dx.doi.org/10.1007/s11249-014-0381-5>.
- [11] Huang HD, Tu JP, Zou TZ, Zhang LL, He DN. Friction and wear properties of IF-MoS₂ as additive in paraffin oil. *Tribol Lett* 2005;20:247–50. <http://dx.doi.org/10.1007/s11249-005-8552-z>.
- [12] Kornaev A, Savin L, Kornaeva E, Fetisov A. Influence of the ultrafine oil additives on friction and vibration in journal bearings. *Tribol Int* 2016;101:131–40. <http://dx.doi.org/10.1016/j.triboint.2016.04.014>.
- [13] Aldana PU, Vacher B, Le Mogne T, Belin M, Thiebaut B, Dassenoy F. Action mechanism of WS₂ nanoparticles with ZDDP additive in boundary lubrication regime. *Tribol Lett* 2014;56:249–58. <http://dx.doi.org/10.1007/s11249-014-0405-1>.
- [14] Aldana PU, Dassenoy F, Vacher B, Le Mogne T, Thiebaut B. WS₂ nanoparticles anti-wear and friction reducing properties on rough surfaces in the presence of ZDDP additive. *Tribol Int* 2016;102:213–21. <http://dx.doi.org/10.1016/j.triboint.2016.05.042>.
- [15] Ratoi M, Niste VB, Alghawel H, Suen YF, Nelson K. The impact of organic friction modifiers on engine oil tribofilms. *RSC Adv* 2014;4:4278–85. <http://dx.doi.org/10.1039/C3RA46403B>.
- [16] Xu Y, Hu E, Hu K, Xu Y, Hu X. Formation of an adsorption film of MoS₂ nanoparticles and dioctyl sebacate on a steel surface for alleviating friction and wear. *Tribol Int* 2015;92:172–83. <http://dx.doi.org/10.1016/j.triboint.2015.06.011>.
- [17] Gustavsson F, Jacobson S. Diverse mechanisms of friction induced self-organisation into a low-friction material – an overview of WS₂ tribofilm formation. *Tribol Int* 2016. <http://dx.doi.org/10.1016/j.triboint.2016.04.029>.
- [18] Bartz WJ, Müller K. Investigations on the lubricating effectiveness of molybdenum disulfide. *Wear* 1972;20:371–9. [http://dx.doi.org/10.1016/0043-1648\(72\)90416-4](http://dx.doi.org/10.1016/0043-1648(72)90416-4).
- [19] Holinski R, Gänsheimer J. A study of the lubricating mechanism of molybdenum disulfide. *Wear* 1972;19:329–42. [http://dx.doi.org/10.1016/0043-1648\(72\)90124-X](http://dx.doi.org/10.1016/0043-1648(72)90124-X).
- [20] Haiden C, Wopelka T, Jech M, Keplinger F, Vellekoop MJ. Sizing of metallic nanoparticles confined to a micro-fluidic film applying dark-field particle tracking. *ACS Publ*; 2014.
- [21] Standard DIN 51347-2 n.d.
- [22] Tannous J, Dassenoy F, Lahouij I, Le Mogne T, Vacher B, Bruhács A, et al. Understanding the tribochemical mechanisms of IF-MoS₂ nanoparticles under boundary lubrication. *Tribol Lett* 2011;41:55–64. <http://dx.doi.org/10.1007/s11249-010-9678-1>.
- [23] Kalin M, Kogovšek J, Remškar M. Mechanisms and improvements in the friction and wear behavior using MoS₂ nanotubes as potential oil additives. *Wear* 2012;280–281:36–45. <http://dx.doi.org/10.1016/j.wear.2012.01.011>.
- [24] Niste VB, Ratoi M. Tungsten dichalcogenide lubricant nanoadditives for demanding applications. *Mater Today Commun* 2016;8:1–11. <http://dx.doi.org/10.1016/j.mtcomm.2016.04.015>.
- [25] Ratoi M, Niste VB, Walker J, Zekonyte J. Mechanism of action of WS₂ lubricant nanoadditives in high-pressure contacts. *Tribol Lett* 2013;52:81–91. <http://dx.doi.org/10.1007/s11249-013-0195-x>.
- [26] Ratoi M, Niste VB, Zekonyte J. WS₂ nanoparticles – potential replacement for ZDDP and friction modifier additives. *RSC Adv* 2014;4:21238. <http://dx.doi.org/10.1039/c4ra01795a>.
- [27] Niste VB, Tanaka H, Ratoi M, Sugimura J. WS₂ nanoadditized lubricant for applications affected by hydrogen embrittlement. *RSC Adv* 2015;5:40678–87. <http://dx.doi.org/10.1039/C5RA03127C>.